Electronic transport properties of single-wall boron nanotubes*

Xinyue Dai(代新月), Yi Zhou(周毅), Jie Li(李洁),
Lishu Zhang(张力舒), Zhenyang Zhao(赵珍阳), and Hui Li(李辉)†

Key Laboratory for Liquid–Solid Structural Evolution and Processing of Materials, Ministry of Education, Shandong University, Jinan 250061, *China*

(Received 6 March 2017; revised manuscript received 21 April 2017; published online 20 June 2017)

Electronic transport properties of single-wall boron nanotube (BNT) with different chiralities, diameters, some of which are encapsulated with silicon, germanium, and boron nanowires are theoretically studied. The results indicate that the zigzag $(3,3)$ BNT has more electronic transmission channels than the armchair $(5,0)$ BNT because of its unique structure distortion. Nanowires encapsulated in the BNT can enhance the conductance of the BNT to some extent by providing a significant electronic transmission channel to the BNT. The effect of the structure of nanowires and the diameter of BNTs on the transport properties has also been discussed. The results of this paper can enrich the knowledge of the electron transport of the BNT and provide theoretical guidance for subsequent experimental study.

Keywords: electronic transport, boron nanoube, BNT

PACS: 73.63.–b **DOI:** 10.1088/1674-1056/26/8/087310

1. Introduction

The low-dimensional structure of the carbon element, such as carbon nanowires, carbon nanotubes (CNTs), graphene, and carbon nanoribbons have attracted a great deal of attention because of their unique structure and special physical properties.[1–3] These carbon materials can be used in nanoscale electron devices.[4,5] However, the properties of CNTs show either conductors or semiconductors depending on their diameters and chirality,[6] which restricts a variety of the promising applications for CNTs. Therefore, it is urgent to seek a new alternative one-dimensional material.

Recently, the nanostructure of the boron element, the neighbor of the carbon element in the periodic table, has arosed a lot of interest because it is predicted to have good properties. Boustani *et al.*[7] firstly studied the boron sheet and boron nanotubes, who found that the BNTs are composed of a triangular lattice or fold triangular lattice. Although this kind of structure is considered to be unstable in later studies, it opened a door to the investigations and applications of BNTs. Ciuparu *et al.*[8] firstly experimentally synthesized the pure BNT, to proved the existence of BNT, but not determine its lattice structure. Since then, much work has been done to predict the lattice structure of BNT, such as the earliest buckled triangular (BT) structure,[9–11] the distorted hexagonal (DH) structure,[12] and mixed triangular-hexagonal (α-sheet, β-sheet) structure.[13–16] Theoretical studies demonstrated that the α-sheet is the relatively stable structure of boron sheet and the nanotubes obtained from the α-sheet agree well with the experiment.[17]

A great deal of advances have been made on the properties of the BNTs. Bezugly *et al.* studied the armchair $(64,0)$ and zigzag $(36,36)$ BNTs derived from the α-sheet, having diameters of 10.2 nm and 9.9 nm respectively and drew the conclusion that they behave as metals.[16] Yang *et al.*[18] studied the zigzag $(7,7)$, $(3,3)$, and armchair $(5,0)$ BNTs, and showed that the $(7,7)$ BNT is metal while the $(5,0)$ and $(3,3)$ BNTs are semiconductors. Singh *et al.*[14] studied a series of BNTs with different diameters and chirality and showed that all the BNTs with smaller diameters are semiconducting regardless of their chirality, while BNTs with the larger diameter are metals. Szwacki *et al.*[19] predicted that all the BNTs obtained from the α-sheet are free from structural distortions; therefore, they are all conductors. Tang *et al.*[20] studied the electronic properties of these nanotubes, and found that small-diameter BNTs are semiconducting and the semiconducting nature is robust under various perturbations and fluctuations. Some researches indicate that nanowires encapsulated in nanotubes can change their performance.[21,22] Choi *et al.*[23] studied the variety of Cu nanowires structure encapsulated in CNTs. Weissmann *et al.*[24] studied the structure and magnetic properties of Fe nanowires encapsulated in CNTs. Zhang *et al.*[25] tried to insert the Si, Ge, Sn nanowires into CNTs to control the performance of CNTs and nanowires.

Despite all of these achievements, investigation of the electrical transport properties of the BNTs is limited for the following reasons. On the one hand, the lattice structure of BNTs still needs to be determined experimentally and even their existence is still debated. On the other hand, the experimental conditions (reactant gases, vacuum condition, nano-

*Project supported by the National Natural Science Foundation of China (Grant No. 51671114) and the Special Funding in the Project of the Taishan Scholar Construction Engineering and National Key Research Program of China (Grant No. 2016YFB0300501).

†Corresponding author. E-mail: lihuilmy@hotmail.com

© 2017 Chinese Physical Society and IOP Publishing Ltd

sized catalyst) of synthesizing the pure BNT is limited.[26–28] While molecular simulation technology can solve these problem. Therefore, detailed study of the electrical transport properties of BNTs is very timely. Thus, the purpose of this work is to use molecular simulations to systematically study the electrical transport properties of the BNTs.

2. Computational method

First-principle computation has been performed by the software package CASTEP, based on the density functional theory (DFT) and pseudopotential plane wave.[29] The generalized gradient approximations (GGA)[30] and Perdew–Burke–Ernzerhof (PBE) change correlation function[31] are used. Special k-point of $2\times2\times4$ were employed. The calculation was run using the ultra-soft pseudopotential (USPs).[32] Geometry optimization calculations have been done to obtain the structure of nanowires encapsulated in BNTs using the module Forcite with the universal force field and the number of the max iterations is 10^5. The energy convergence tolerance and force convergence tolerance are defined as 0.001 kcal/mol and 0.5 kcal/mol·Å respectively to guarantee the accuracy of the calculation.[25]

The quantum electrical transport properties of these BNTs are obtained by a self-consistent calculation based on the nonequilibrium Green function (NEGF) and extended Huckel theory (EHT)[33] using the Atomistix ToolKit software package (ATK). Special k-points of $1\times1\times100$ were employed. Au (111) films are used as contacts. The schematic representation of the device of BNTs is shown in Fig. 1. Yuan *et al.*[34] studied the electronic transport properties of composite nanotubes with and without Au (111) electrodes. The results indicate that if the chirality of the composite nanotubes is the same, the contacts between tube and Au (111) electrodes have minor impact on the transport properties. However, if the composite nanotubes have different chirality, more chemical bonds formed between the ultrathin nanotubes and metal electrodes can help to increase the transmission. This work plays an important role in choosing the contaction types between nanotubes and Au (111). The contact type in this work can form more B-Au connections to improve the contact quality between the BNT and Au (111) surface, which is similar to the composite nanotubes and Au (111).

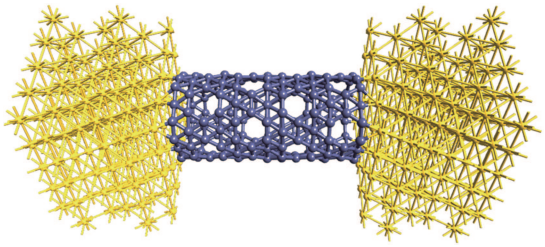


Fig. 1. (color online) Schematic representation of the contact-nanotube-contact system.

In this calculation, BNT-Au (111) contact distance is constant when BNTs changed. The vertical distance between the end atoms of the BNT and the Au contacts is set to 1.811 Å. The length of BNT is equal to 10 B–B bonds length (17 Å).

The transmission T is a measure of probability of electrons transmitting from the source to the drain contacts through the BNT and it can be shown as follows:

$$T(E,V) \equiv \mathrm{tr}\left(\Gamma_1 G \Gamma_2 G^{\dagger}\right),$$

where G and $G^{\dagger}$ are the retarded and advanced Green functions of the conductor part and Γ_1 and Γ_2 are the coupling functions to the left and right electrodes. The density of states $D(E)$ is given as:

$$D(E) \equiv \frac{\mathrm{tr}\left(\mathrm{i}\left(G-G^{\dagger}\right)S\right)}{2\pi},$$

where the overlap matrix S is used to describe the electronic structure of the BNT.

3. Result and discussion

3.1. Influence of chirality

Figure 2 shows the equilibrium (zero-bias) transmission spectrum and density of states of the $(5,0)$ and $(3,3)$ BNTs, whose average diameters are equal to 8.5 Å. The insets in Figs. 2(a) and 2(b) illustrate the top view of unrelaxed (pink one) and relaxed (grey one) $(5,0)$ and $(3,3)$ BNTs. The top view of optimized BNT becomes an irregular circle with deformation in the center of the hexagonal grid. However, for $(5,0)$ BNT, the curvature effect is smaller (shown in Fig. 2(a)). As we know, electrical conductance is determined by the states around the Fermi energy. It is obvious that there is an obvious peak near the Fermi level (at -0.08 eV) in the curve of equilibrium transmission spectrum for the $(3,3)$ BNT, which corresponds to the peak in the curve of density of states, as shown in Fig. 2(d). The density of states can be seen as a visualization result of the band structure. From the density of states for $(5,0)$ and $(3,3)$ BNTs, we can see that the pseudogap of the $(5,0)$ BNT is wider than the $(3,3)$ BNT, indicating its stronger covalent nature. The peak at -1.2 eV in the density of states shows the electronic localization characteristics of the $(5,0)$ BNT. Obviously, the chirality of BNTs with small diameter have some effect on their electronic transport properties. The effect of chirality may be explained by the difference of the structure deformation.

Furthermore, there is no energy gap at the Fermi energy in the DOS, indicating a typical metallic behavior. The insets in Figs. 2(c) and 2(d) show the transmission channels at the Fermi level of the $(5,0)$ and $(3,3)$ BNTs. It can be concluded that, for the $(5,0)$ BNT, the electric current flows along

the only spiral electronic transmission channel on the surface. While for the (3,3) BNT, the electric current flows along the whole surface of the nanotube. That is to say, the (3,3) BNT has more electronic transmission channels than (5,0) BNT because of its zigzag structure. In the transmission channels of the (3,3) and (5,0) BNTs, B-s and B-p orbital hybridization forms a π bond. Jain *et al.*[35] studied the band structure and density of states for different BNTs with different chiralities, and suggested that the conductance of the zigzag BNT should be higher than the armchair BNT.

The band structure and Bloch states for the (5,0) and (3,3) BNTs are shown in Figs. 3 and 4, respectively. It can be seen from their band structures that both of them are metallic, but their electronic structure is different. For the (5,0) BNT, there are two bands crossing the Fermi level. The corresponding bloch states at the Γ point (shown in Figs. 3(b) and 3(d)) distribute at the whole surface of BNT, and at the Z point (shown in Figs. 3(c) and 3(e)) tend to move to the edge of the BNT. For the (3,3) BNT, there are three bands crossing the Fermi level. The Bloch states of the two bands nearest to the Fermi level are shown in Figs. 4(b)–4(e). Different with the (5,0) BNT, the bloch states of the (3,3) BNT are more noticeable but localized at several atoms of the BNT. The bands for the (5,0) BNT are more narrow than the (3,3) BNT and the fluctuation of them is smaller, indicating the electronic localization characteristics of the (5, 0) BNT.

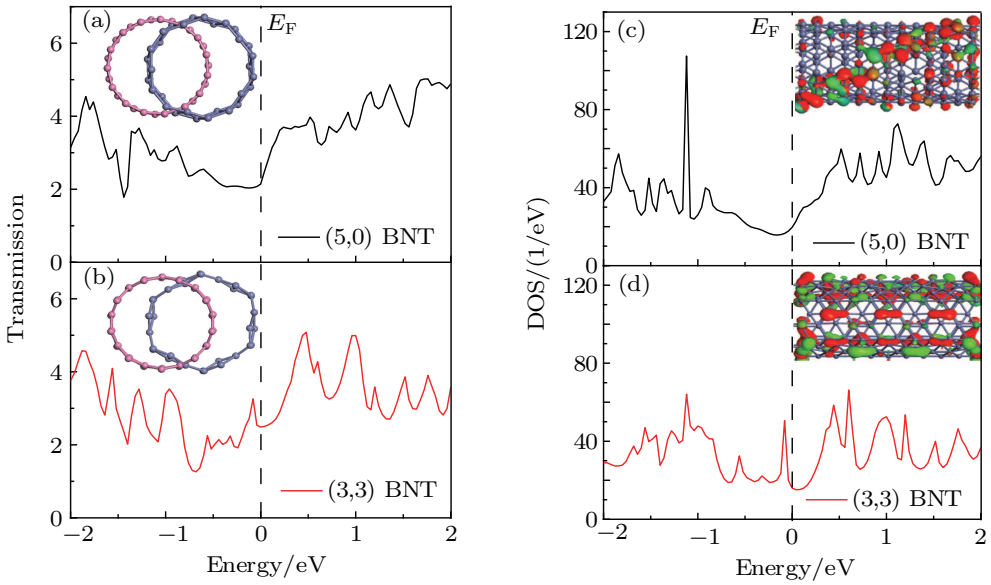


Fig. 2. (color online) Electronic transmission properties of armchair (5,0) and zigzag (3,3) BNTs. (a) Equilibrium transmission spectrum for (5,0) BNT, the inset illustrates the top view of (5,0) BNT. (b) Equilibrium transmission spectrum for (3,3) BNT, the inset illustrates the top view of (3,3) BNT. (c) Density of states for (5,0) BNT, the inset illustrates the transmission channel at the Fermi level with eigenvalues of 0.8772. (d) Density of states for (3,3) BNT, the inset illustrates the transmission channel at the Fermi level with eigenvalues of 0.9611. The Fermi level is set to zero.

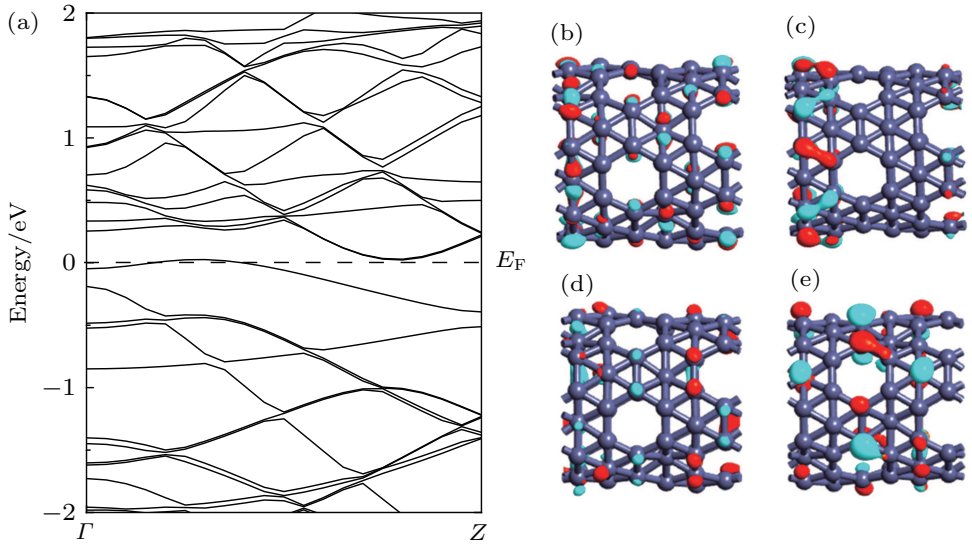


Fig. 3. (color online) The band structure and Bloch states of the band 118 at the Γ point (b) and at the Z point (c) and band 119 at the Γ point (d) and at the Z point (e) for the armchair (5,0) BNT with an isovalue of 0.035.

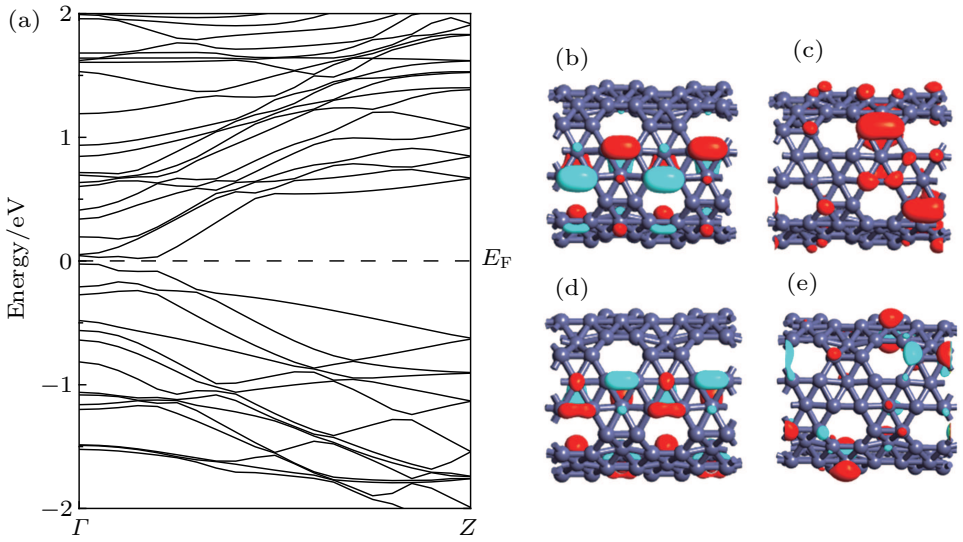


Fig. 4. (color online) The band structure (a) and Bloch states of the band 143 at the Γ point (b), and at the Z point (c) and band 144 at the Γ point (d) and at the Z point (e) for the zigzag $(3,3)$ BNT with an isovalue of 0.035.

3.2. Influence of nanowires

Figures 5(a)–5(c) despict the electronic transport properties of the $(5,0)$ BNT encapsulated with silicon, germanium and boron nanowires respectively. The insets illustrate the optimized geometries of these BNTs. These nanowires are all monoatomic chains but have different effects on the electronic transport properties of the $(5,0)$ BNT. It can be seen that, around the Fermi energy, the $(5,0)$ BNT inserted by silicon nanowire has the largest transmission, indicating that silicon nanowire encapsulated in the $(5,0)$ BNT can improve the electrical conductivity of the $(5,0)$ BNT.

Figures 5(d)–5(f) show the electronic transport properties of the $(3,3)$ BNT encapsulated with silicon, germanium, and boron nanowires respectively. Similar to the $(5,0)$ BNT, these nanowires are all monoatomic chains and have different effects on the electronic transport properties of BNT. Interestingly, around the Fermi energy, the $(3,3)$ BNT inserted by boron nanowire has the biggest transmission value, showing that, boron nanowire in the $(3,3)$ BNT has more significant effect on its electronic transport properties rather than Si and Ge, which is quite different with the $(5,0)$ BNT.

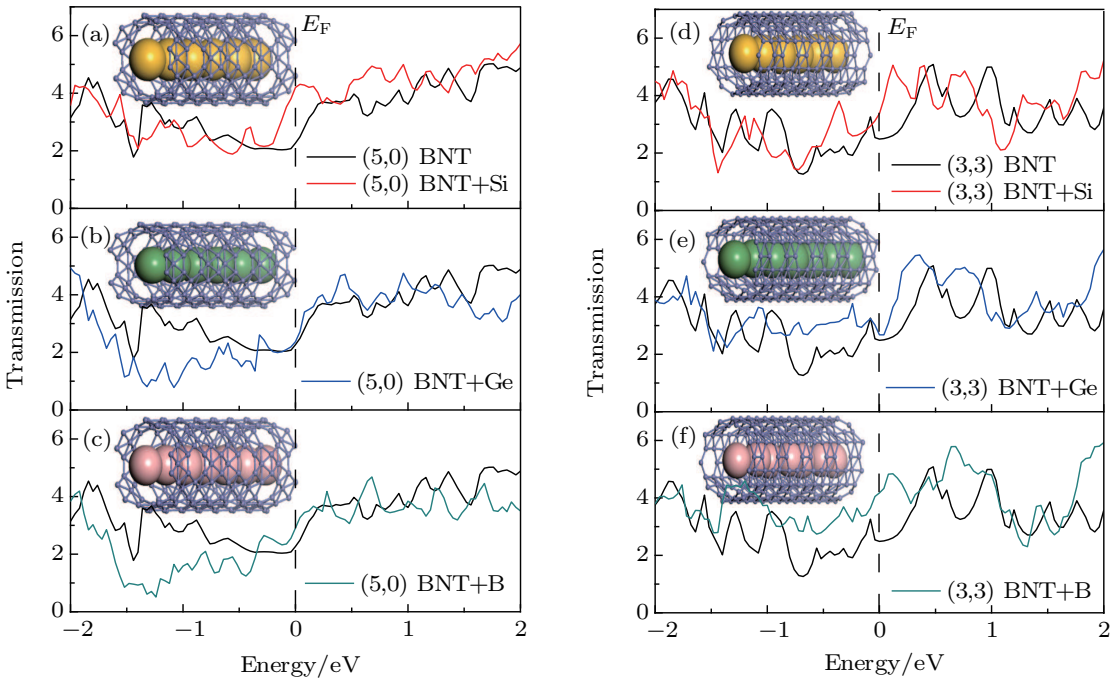


Fig. 5. (color online) Equilibrium transmission spectrum for the armchair $(5,0)$ BNT encapsulated with silicon (a), germanium (b), and boron (c) nanowires and zigzag $(3,3)$ BNT encapsulated with silicon (d), germanium (e), and boron (f) nanowires. The insets illustrate the structure of these BNTs respectively. The Fermi level is set to zero.

As far as these three nanowires are concerned, silicon nanowire can improve not only the electrical conductivity of the $(5,0)$ boron nanotube, but also enhance the electrical conductivity of the $(3,3)$ boron nanotube around the Fermi energy. Germanium nanowire has some effect on the electronic transport properties of the $(3,3)$ boron nanotube but not on the $(5,0)$ boron nanotube. Boron nanowire can improve the electrical conductivity of the $(3,3)$ more greatly than that of the $(5,0)$ boron nanotube.

Figure 6 shows the partial density of states for the armchair $(5,0)$ boron nanotube encapsulated with the silicon nanowire. The electron transmission spectrums are responsible for the electronic states. Near the 0.5 eV, the value of density of states mainly due to the Si-p orbital, with a minor contribution of tube-p and tube-s orbitals. The electronic structure indicates the hybridization of the B-s, B-p, and Si-p orbitals, which corresponds to the interaction between the $(5,0)$ boron nanotube and the silicon nanowire.

Figure 7 shows the partial density of states for the zigzag $(3,3)$ boron nanotube encapsulated with the boron nanowire. This figure indicates that the orbital contributions in the density of states of the $(3,3)$ boron nanotube encapsulated with the boron nanowire are similar to the $(5,0)$ boron nanotube encapsulated with the silicon nanowire. At -0.2 eV and 0.3 eV, the position of peaks of B-p and B-s orbitals is consistent, which shows the hybridization of B-s and B-p orbitals, indicating that the interactions within these atomic orbitals of the nanowires give a significant contribution to the total density of states.

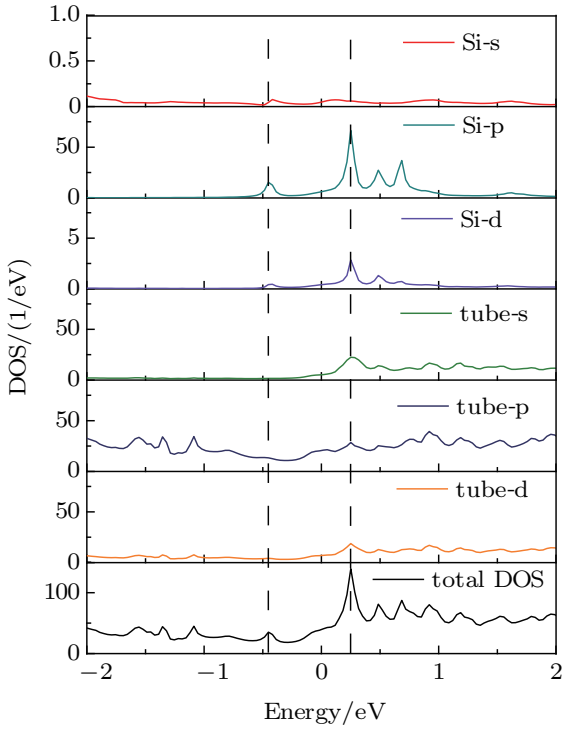


Fig. 6. (color online) Partial density of states for armchair $(5,0)$ boron nanotube encapsulated with the silicon nanowire. The Fermi level is set to be zero.

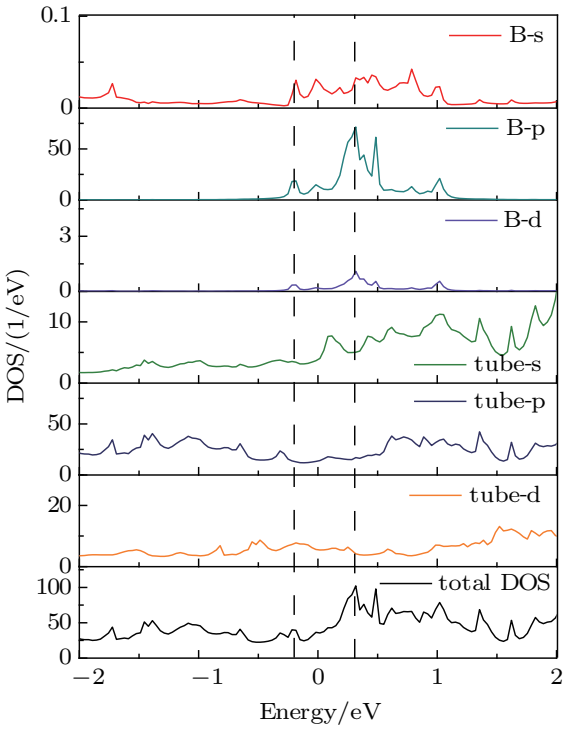


Fig. 7. (color online) Partial density of states for zigzag $(3,3)$ boron nanotube encapsulated with the boron nanowire. The Fermi level is set to be zero.

3.3. Influence of diameters

Figure 8 shows the equilibrium (zero-bias) transmission spectrum and density of states of the $(6,0)$ and $(4,4)$ BNTs encapsulated with the silicon nanowire.

Obviously, with the diameter of the BNTs increasing continuously, the structure of nanowires varies from monoatomic chain, to double helical chain, and three-spiral chain. Silicon nanowire formed in the $(3,3)$ BNT, whose diameter is 8.5 Å, is monoatomic chain and the electronic transport properties of the BNT have smaller increments (as shown in Fig. 5(d)). The silicon nanowire formed in the $(6,0)$ BNT, whose diameter is 10.189 Å, is the double helix chain and has some effect on the electronic transport properties of the BNT (as shown in Fig. 8(a)). The silicon nanowire formed in the $(4,4)$ BNT, whose diameter is 11.409 Å, is the three-spiral chain and can improve the electrical conductivity of the BNT around the Fermi energy (as shown in Fig. 8(c)).

The insets in Figs. 8(b) and 8(d) show that the transmission channels at the Fermi level of the $(6,0)$ and $(4,4)$ BNTs encapsulated with the silicon nanowire confirm that the silicon nanowire can provide a significant electronic transmission channel to the BNT, and thus enhance its conductance.

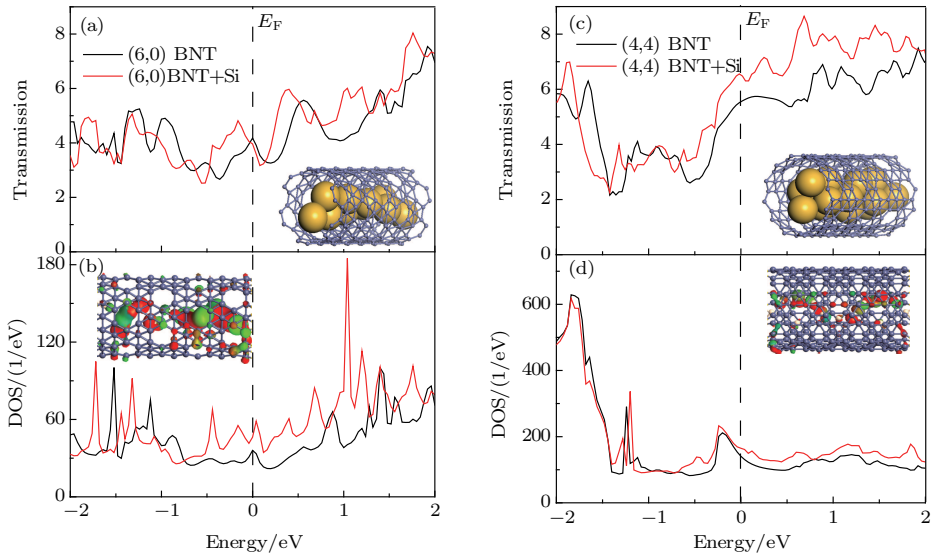


Fig. 8. (color online) Electronic transmission properties of the armchair $(6,0)$ and zigzag $(4,4)$ BNTs encapsulated with the silicon nanowire. (a) Equilibrium transmission spectrum for $(6,0)$ BNT encapsulated with the silicon nanowire, the inset is its geometric structure. (b) Density of states for the $(6,0)$ BNT encapsulated with the silicon nanowire, the inset illustrates the transmission channel at the Fermi level with eigenvalues of 0.8373. (c) Equilibrium transmission spectrum for the $(4,4)$ BNT encapsulated with silicon nanowire, the inset is its geometric structure. (d) Density of states for the $(4,4)$ BNT encapsulated with the silicon nanowire, the inset illustrates the transmission channel at the Fermi level with eigenvalues of 0.9972. The Fermi level is set to be zero.

4. Conclusions

Electronic transport properties of single-wall boron nanotubes encapsulated with silicon, germanium, and boron nanowires have been studied by using a self-consistent calculation based on the EHT and NEGF. The results indicate that the electronic transport properties of BNTs are related to their chirality and diameter. First, the zigzag $(3,3)$ BNT has more electronic transmission channels than the armchair $(5,0)$ BNT because of its unique structure distortion. Second, nanowires encapsulated in the BNT can enhance the conductance of the BNT to some extent by providing a significant electronic transmission channel to the BNT. The extra transmission channel is mainly composed of p orbitals of the atoms in nanowire. This work provides insight into the electronic transport properties of BNTs.

References

[1] Bockrath M, Cobden D H, McEuen P L, Chopra N G, Zettl A, Thess A and Smalley R E 1997 *Science* **275** 1922

[2] Bachilo S M, Strano M S, Kittrell C, Hauge R H, Smalley R E and Weisman R B 2002 *Science* **298** 2361

[3] Chen Y, Zhang H, Liu X G, Xia L S and Yang A M 2011 *Acta Phys. Sin.* **60** 080702 (in Chinese)

[4] Baughman R H, Zakhidov A A and de Heer W A 2002 *Science* **297** 787

[5] Tans S J, Verschueren A R and Dekker C 1998 *Nature* **393** 49

[6] Dresselhaus M S, Dresselhaus G and Jorio A 2004 *Ann. Rev. Mater. Res.* **34** 247

[7] Boustani I and Quandt A 1997 *Europhys Lett.* **39** 527

[8] Ciuparu D, Klie R F, Zhu Y and Pfefferle L 2004 *J. Phys. Chem. B* **108** 3967

[9] Gindulyte A, Lipscomb W N and Massa L 1998 *Inorg. Chem.* **37** 6544

[10] Sebetci A, Mete E and Boustani I 2008 *J. Phys. Chem. Solids* **69** 2004

[11] Kunstmann J and Quandt A 2006 *Phys. Rev. B* **74** 35413

[12] Zhang D, Zhu R and Liu C 2006 *J. Mater. Chem.* **16** 2429

[13] Kunstmann J, Bezugly V, Rabbel H, Mmeli M H and Cuniberti G 2014 *Adv. Funct. Mater.* **24** 4127

[14] Tang H and Ismail-Beigi S 2007 *Phys. Rev. Lett.* **99** 115501

[15] Singh A K, Sadrzadeh A and Yakobson B I 2008 *Nano Lett.* **8** 1314

[16] Yu X, Li L, Xu X and Tang C 2012 *J. Phys. Chem. C* **116** 20075

[17] Bezugly V, Kunstmann J, Grundkotter-Stock B, Frauenheim T, Niehaus T and Cuniberti G 2011 *ACS Nano* **5** 4997

[18] Yang X, Ding Y and Ni J 2008 *Phys. Rev. B* **77** 041402

[19] Szwacki N G and Tymczak C J 2010 *Chem. Phys. Lett.* **494** 80

[20] Tang H and Ismail-Beigi S 2010 *Phys. Rev. B* **82** 115412

[21] Cao H Q, Xu Z, Sang H, Sheng D and Tie C Y 2001 *Adv. Mater.* **13** 121

[22] Bao J, Xu D, Zhou Q, Xu Z, Feng Y and Zhou Y 2002 *Chem. Mater.* **14** 4709

[23] Choi W Y, Kang J W and Hwang H J 2003 *Phys. Rev. B* **68** 193405

[24] Weissmann M, Garc I A G, Kiwi M, Ram I Rez R and Fu C 2006 *Phys. Rev. B* **73** 125435

[25] Zhang X Q, Li H and Liew K M 2007 *J. Appl. Phys.* **102** 73709

[26] Patel R B, Chou T and Iqbal Z 2015 *J. Nanomater.* **16** 14

[27] Patel R B 2013 *Synthesis and characterization of novel boron-based nanostructures and composites* (New Jersey: Institute of Technology)

[28] Liu J and Iqbal Z 2011 *MRS Proceedings* (Cambridge: Cambridge University Press) p. mrsf10-1307

[29] Payne M C, Teter M P, Allan D C, Arias T A and Joannopoulos J D 1992 *Rev. Mod. Phys.* **64** 1045

[30] Perdew J P, Burke K and Ernzerhof M 1996 *Phys. Rev. Lett.* **77** 3865

[31] Perdew J P, Burke K and Wang Y 1996 *Phys. Rev. B* **54** 16533

[32] Vanderbilt D 1990 *Phys. Rev. B* **41** 7892

[33] Zienert A, Schuster J and Gessner T 2013 *J. Phys. Chem. A* **117** 3650

[34] Yuan J, Hu Y, Liao J, Zhong J and Mao Y 2016 *Mater. Design* **95** 641

[35] Jain S K and Srivastava P 2011 *Comput. Mater. Sci.* **50** 3038